

Structural and electrical properties of STF materials for SOFC applications

MATEUSZ TOLCZYK¹, SEBASTIAN MOLIN², MARIA GAZDA¹, PIOTR JASINSKI²

¹ Faculty of Applied Physics and Mathematics, Gdańsk University of Technology, Gdańsk, Poland

² Faculty of Electronics, Telecommunications and Informatics, Gdańsk University of Technology, Gdańsk, Poland
e-mail: molin@biomed.eti.pg.gda.pl

Abstract

In this study, iron doped strontium titanates (STF) are considered as possible SOFC cathode materials in the temperature range of 600-800°C. Their synthesis, electrochemical and structural parameters are evaluated. Electrochemical performance analysis is performed by means of the Electrochemical Impedance Spectroscopy on symmetrical cells sintered at different temperatures. Chemical interaction of STF materials with yttria stabilized zirconia solid electrolyte is considered by the X-ray diffractometry analysis of reacted powders. Comparison with available data is presented and discussed.

Keywords: SOFC, Strontium titanates, Electrochemical properties, Microstructure - final

WŁAŚCIWOŚCI STRUKTURALNE I ELEKTRYCZNE MATERIAŁÓW STF DO ZASTOSOWAŃ W SOFC

Tytaniany strontu domieszkowane żelazem (STF) rozważane są jako potencjalne materiały katodowe w SOFC do pracy w temperaturach z przedziału 600-800°C. Ich synteza, właściwości elektrochemiczne i strukturalne są oceniane. Analizę wydajności elektrochemicznej przeprowadzono za pomocą elektrochemicznej spektroskopii impedancyjnej na symetrycznych komórkach spieczonych w różnych temperaturach. Wzajemne oddziaływanie chemiczne materiałów STF i cyrkonowego elektrolitu stalego stabilizowanego tlenkiem itru bada się za pomocą dyfraktometrii rentgenowskiej reagujących proszków. Prezentuje się i dyskutuje porównanie z dostępnymi danymi.

Słowa kluczowe: SOFC, tytaniany strontu, właściwości elektrochemiczne, mikrostruktura finalna

1. Introduction

Solid Oxide Fuel Cells (SOFCs) are solid state energy conversion devices which have attracted much attention [1]. Their main advantages are very high efficiencies of energy conversion and broad range of fuels that can be used. Also due to operation at elevated temperatures, usually between 800-1000°C, high electrode efficiencies can be achieved. Possibility of obtaining high efficiencies is connected with the lack of the combustion phase, which exists in internal combustion engines. Conversion from the fuel energy into the electrical energy and heat release occurs in an electrochemical manner without combustion phase and mechanical conversion does not occur. Current research trend is in lowering the operating temperature of SOFC to the intermediate temperature range, *i.e.*, 600-800°C. At lowered temperatures cheaper materials might be used for SOFC fabrication, but on the other hand electrochemical performances of electrolyte and electrodes are reduced and thus new materials must be developed. In the case of the electrolyte, for which an increase of ohmic resistance is the main problem, the compensation for lowering temperature may be achieved by the application of a thinner electrolyte [2]. In case of the electrodes the electrochemical performance is lowered due to rather sluggish chemical kinetics

(chemical resistance) of oxygen reduction reaction (ORR), surface exchange kinetics, etc. [3].

A perovskite family of materials are almost exclusively used for cathode fabrication. The family is recognized by general chemical formula of ABO_3 , which can be easily doped on A and B site and thus the properties of perovskite can be altered. For many years a $(La,Sr)MnO_3$ (LSM) cathode have gained broad popularity [4]. This material has been applied to many fuel cells and its physicochemical properties are well documented and available in literature. Main drawback of this material is the fact of only electronic nature of the conductivity. It must be mixed with good ionic conductor to form a mixed conductor (MIEC – mixed ionic electronic conductor), for which higher electrochemical performances can be achieved. Due to these requirements new MIEC electrode materials have been found and used. These include especially $(La,Sr)(Co,Fe)O_3$ (LSCF) group, which reveal high oxygen ionic conductivity and good level of electronic conductivity.

Strontium titanate $SrTiO_3$ (STO) has a perovskite crystal structure and can be easily doped in a broad range. It is stable at high temperatures and has been extensively studied due to its dielectric properties. In its undoped state it has rather low conductivity and is a wide-bandgap semiconductor with $E_g = 3.2$ eV at 0 K [5]. It can be either acceptor or donor doped

to meet many possible demands. Successful applications for resistive oxygen gas sensors have been presented with Nb doped STO [6]. For Solid Oxide Fuel Cells this material can be used for an anode [7-9]. Nb doped STO has shown very good electrochemical performance when compared to the standard anode material of choice: the Ni-YSZ cermet. Iron doped strontium titanates, $\text{SrTi}_{1-x}\text{Fe}_x\text{O}_{3\pm\delta}$ (STF), are promising materials for resistive-type oxygen gas sensors [5, 10, 11]. Also a propane gas sensor operating in the temperatures below 500°C was constructed using this material [12]. Their composition can be tailored to have a zero temperature coefficient of resistivity, *i.e.*, their conductivity is independent of temperature in some temperature range (zero-TCR: zero-temperature coefficient of resistivity).

Table 1. Electrochemical and electrical properties of perovskites considered as SOFC cathodes. Data taken from [13]. Values given for 800°C.

Material	Surface exchange	σ_{el}	σ_{ion}	t_{el}
–	[$\text{cm}\cdot\text{s}^{-1}$]	[$\text{S}\cdot\text{cm}^{-1}$]	[$\text{S}\cdot\text{cm}^{-1}$]	–
STF5	$1.2\cdot 10^{-5}$	$4.5\cdot 10^{-3}$	$5.7\cdot 10^{-4}$	0.88
STF10	$1.4\cdot 10^{-5}$	$1.4\cdot 10^{-2}$	$1.7\cdot 10^{-3}$	0.89
STF35	$2.0\cdot 10^{-5}$	$9.9\cdot 10^{-1}$	$3.5\cdot 10^{-2}$	0.96
STF50	$1.7\cdot 10^{-5}$	1.8	$3.6\cdot 10^{-2}$	0.97
LSCF	$5.6\cdot 10^{-6}$	$3.0\cdot 10^2$	$8.0\cdot 10^{-3}$	0.99

By choosing an appropriate level of iron doping, their electrical properties: electronic/ionic conductivity ratio (transference number) can be changed. SrFeO_3 and SrTiO_3 form solid solutions at all compositions. STF materials are proposed as next generation oxygen sensors for exhaust gas monitoring in cars. Recently this material was used by Jung *et al.* as a model mixed conductor cathode material for SOFC application [13, 14]. In their study this material was fabricated in the dense form via Pulsed Laser Deposition (PLD) on the YSZ single crystal with (100) orientation. Deposited layers exhibited a preferred (110) orientation as detected by X-ray diffractometry with grain sizes in the range of 100-200 nm. Thicknesses of these dense electrodes were 70-440 nm. In the temperature range of 570–650°C this material has shown very low Area Specific Resistance (ASR) even when compared to current state of the art cathodes like $(\text{La,Sr})(\text{Co,Fe})\text{O}_3$ (LSCF) [15] and $(\text{Ba,Sr})(\text{Co,Fe})\text{O}_3$ (BSCF) [16]. The ASR as low as $3\ \Omega\text{cm}^2$ at 650°C for STF80 was reported. A comparison of the surface exchange coefficient and electrical conductivity data of several STF materials with LSCF material are included in the Table 1. [13]. It is apparent that all materials of the STF family have higher surface exchange rates. This parameter is crucial when considering cathode materials, because high surface exchange results in a possible high flux of oxygen ions. Other important features are electronic and ionic conductivities. As can be seen in the Table 1, the substitution of Ti by Fe results in an increase in electronic and ionic conductivities and a decrease in the band gap. Ionic transference number also increases with the increase of iron content. Although the ionic and electronic conductivities increase, the electronic conductivity remains on a low level ($\sim 1\ \text{S}\cdot\text{cm}^{-1}$), which can be insufficient for efficient current collection.

This paper offers the preliminary study of $\text{Sr}(\text{Ti,Fe})\text{O}_3$ materials as the potential SOFC cathode candidate. Three different compositions are evaluated with respect to the Area Specific Resistance and the chemical interaction with the YSZ electrolyte.

2. Experimental procedure

A solid-state synthesis route was chosen as fabrication method of STF powders. Dried powders of SrCO_3 , TiO_2 and Fe_2O_3 (reagent grade, Sigma-Aldrich USA) were used to prepare $\text{SrTi}_{1-x}\text{Fe}_x\text{O}_{3\pm\delta}$ materials with $x = 0.35, 0.50$ and 0.65 . Throughout the text samples, which are described as STF35 have a chemical formula of $\text{SrTi}_{0.65}\text{Fe}_{0.35}\text{O}_3$, STF50 – $\text{SrTi}_{0.50}\text{Fe}_{0.50}\text{O}_3$ and STF65 – $\text{SrTi}_{0.35}\text{Fe}_{0.65}\text{O}_3$. Similar convention is used in reference to samples prepared by other authors. Powders, after initial weighting, were ball milled (Fritsch Pulverisette 7) for 6 hours using ZrO_2 balls and ethanol media. Ball milled powders were pressed into pellets in a steel die and calcined at 1100°C for 4 hours in a muffle furnace. After this step the powders were ball-milled again for 10 hours, re-pressed into pellets and calcined at 1350°C for 2 hours. Next the powders were ball milled again and the resulting powder was analysed by X-ray diffractometry and used for further experiments. Pellets of STF were then pressed at 200 MPa and sintered at 1400°C for 8 hours to obtain dense samples for an electrical conductivity evaluation. Some samples were prepared directly from not reacted reagents that were instantly sintered at 1400°C for 2 hours. This was performed to compare the influence of the powder fabrication route on the resulting properties. Electrical conductivity of these samples was measured by the van der Pauw method. Ag paste (5542, DuPont) was used to prepare 4 contacts on circular samples. YSZ substrates for the symmetrical electrode deposition were prepared by uniaxial die-pressing of a commercial YSZ powder (HSY-8, DKKK, Japan) under a pressure of 200 MPa and sintered at 1450°C for 4 hours. Sample microstructure was analyzed by scanning electron microscope FEI-Philips XL30 ESEM. X-ray diffractometry studies were performed on a Philips X'Pert Pro diffractometer with $\text{CuK}\alpha$ radiation. Sample surfaces were scanned in a standard 2θ configuration at room temperatures. Impedance Spectroscopy studies were performed using a Novocontrol Alpha A mainframe with ZG4 4-wire interface. Excitation voltage of 50 mV and the frequency range from 1.0 MHz to 0.1 Hz was applied. Electrodes were prepared in a symmetrical configuration by brush painting pastes prepared from appropriate STF powders mixed with a vehicle (ESL 401, USA). Diameter of electrodes was 10 mm. The STF symmetrical electrodes on YSZ support were sintered at 1100-1300°C for 1 hour in the static air atmosphere. Heating and cooling rates were 3°C/min. These symmetrical cells were tested in a 4 wire spring loaded test rig with platinum meshes in contact with STF electrodes. Samples were measured in the 800°C to 600°C temperature range with 50°C decrements. STF and YSZ chemical interaction were determined by mixing the STF and YSZ powders in a 30:70 volume ratio and pressed into pellets under a pressure of 200 MPa, which were sintered at 1100-1300°C for 1 hour. After sintering pellets were grounded

in an agate mortar and the resulting powder was analyzed by X-ray diffractometry.

3. Results and discussion

To obtain phase pure STF powders a two stage solid state synthesis method was necessary to perform. The properties of samples after each synthesis step were tested by X-ray diffractometry and by DC electrical conductivity measurements. Unfortunately, the quality of the samples prepared by direct synthesis of reactant oxides and carbonates were not satisfactory. They did not exhibit a zero TCR, which is the characteristic feature of these materials. Therefore a second calcination step was needed and samples prepared from these powders were phase pure and exhibit a conductivity level in very good agreement with the available literature data. After final sintering of samples porosities were higher than 93 %. In comparison to [17] no A-site deficiency was introduced in this work, which probably could improve powders synthesis procedure and long term stability. Only cubic perovskite structure (space group Pm3m) was observed for these powders. It was noticed before, that STF phase pure powders and pellets can be hard to obtain during synthesis and therefore different approaches were considered for fabrication phase pure samples [12]. The results of measurement of DC electrical conductivity of samples prepared from doubly calcined powders are shown in Fig. 1. Measurements were performed in the static air atmosphere. It can be seen that the STF35 sample has a constant level of the electrical conductivity in the temperature range of 750–900°C. The conductivities of the STF50 and STF65 samples are not constant at tested temperatures. At 900°C it was obtained 6.01 Scm⁻¹, 1.69 Scm⁻¹, 0.41 Scm⁻¹ for STF65, STF50 and STF35, respectively. The type of conductivity for STF65 and STF50 is different than for STF35. While STF 35 has a semiconductor-type behaviour, two other compositions show metallic-type behaviour. Similarly, in [18] the resistance of STO and STF35 decreased with the increase of the temperature. Interestingly, the behaviour of STF60 was different for sample prepared by ball-milled and not ball-milled powder. For ball-milled STF60 a metallic type conductivity was reported. The change in this behaviour can be also described by the TCR parameter. As described in [19], due to the different level of the bandgap the TCR value is negative for STF solutions at low Fe content (< 30 %) and changes to positive values at higher Fe concentrations (> 40 %), with zero TCR at intermediate compositions (~35 % Fe). The composition of STF35 having the desired zero-TCR parameter is generally in agreement with the literature data. In [19] it was found that the same composition fulfils the zero-TCR criteria, while in [20] a STF60 has been studied. These small differences can be attributed to some differences in the preparation of powders, *i.e.*, solid state synthesis or self-propagating high-temperature synthesis (SHS) synthesis.

Scanning electron microscopy images of the STF65 cathode on the YSZ, which were subjected to electrical measurements, are shown in Fig. 2. Thickness of the electrode is about 5 µm. Surface of the electrolyte is uniformly covered with electrode material over all electrode area. The cathode remained attached to YSZ even after the measurement and subsection to the mechanical contact of the test rig,

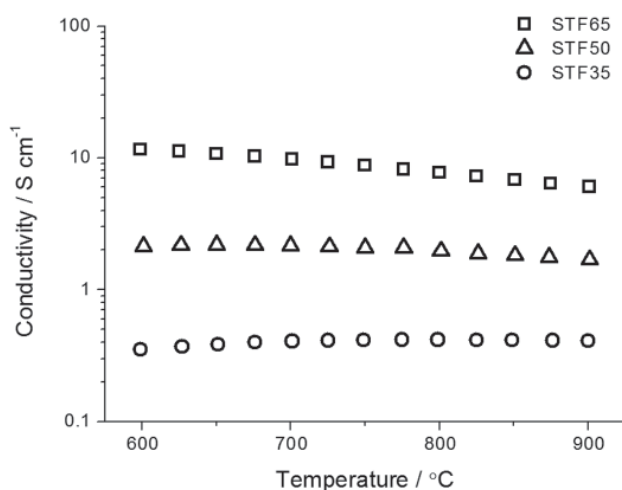


Fig. 1. DC electrical conductivity of STF35, STF50, STF65 pellets measured in air.

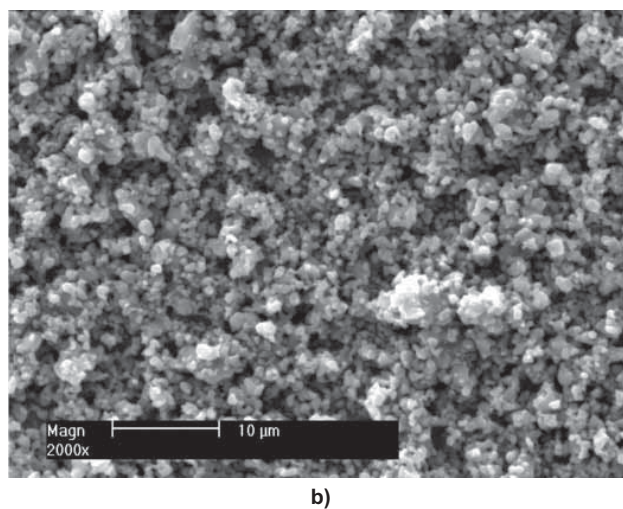
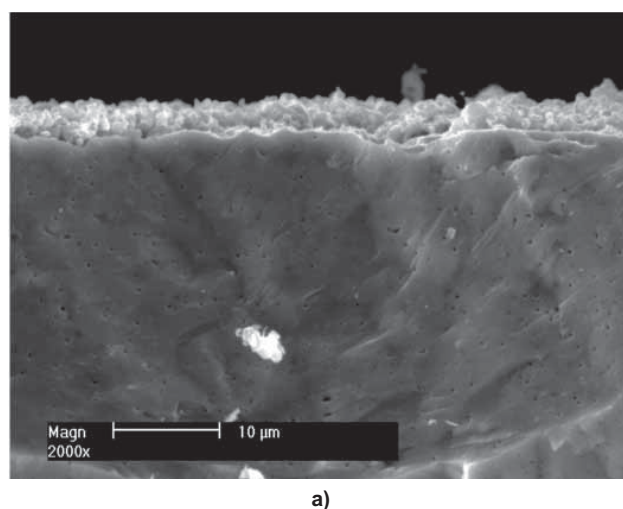


Fig. 2. Scanning Electron Microscope image of the cross section (a) and surface (b) of the STF65 cathode on YSZ surface. Cathode material was sintered at 1100°C for 1 hour.

which implies that electrode material is well adhered to the underlying substrate. Cathode paste was in this case sintered at the lowest temperature studied (1100°C) for 1 hour. The grain size of the STF65 can be approximated to be < 1 µm. Based on surface analysis (Fig. 2b) a high level of porosity

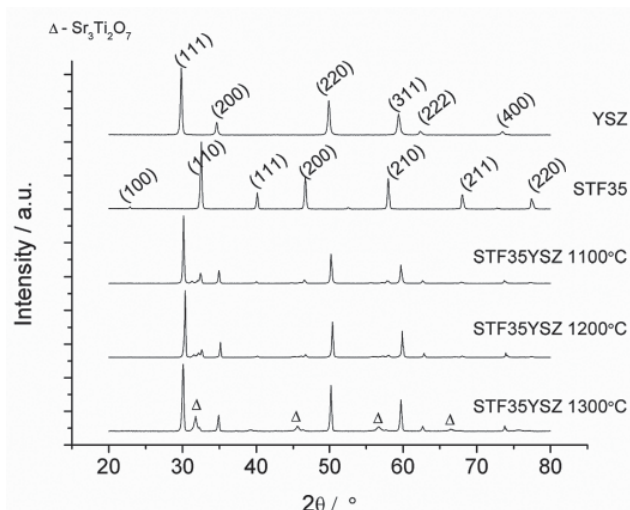


Fig. 3. XRD patterns of the unreacted YSZ, STF35 and their mixture reaction products after exposure to different temperatures.

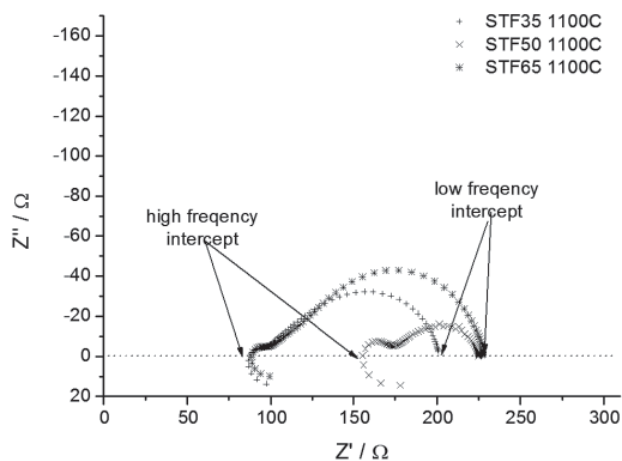


Fig. 4. Impedance spectra measured at 800°C for STF symmetrical electrodes on YSZ sintered at 1100°C for 1 hour.

is observed which is needed to ensure easy gas permeation of the fuel cell cathode.

The chemical interaction between STF and YSZ materials were studied for phase pure STF powders. A successful candidate for SOFC cathode material should sustain a high temperature synthesis of a ceramic paste applied on electrolyte without degradable interaction. Temperature range being considered in this study is 1100°C to 1300°C.

To assess the chemical interaction between the YSZ electrolyte material and STF cathode material, STF powders were mixed with YSZ electrolyte material in a 30:70 volume ratio and then calcined at 1100-1300°C for 1 hour. During the high temperature exposure a reaction between powders takes place. X-ray diffractometry patterns of YSZ, STF and the resulting STF/YSZ reaction products for the STF35 composition are shown in Fig. 3. In case of YSZ measured XRD patterns resembles a fully stabilized cubic zirconia structure (JCPDS number 30-1468). As can be seen in the all sample spectra, YSZ phase is always present, all peaks are clearly visible. The peaks from STF35 material are highly diminished. This can be explained by the smaller amount of the STF material in comparison to the YSZ material. Another reason for the smaller amount of the STF phase is its chemical reaction. Starting at 1100°C only minor new phase is present at

about $2\theta = 31.6^\circ$. Still the most intense ($2\theta = 32.6^\circ$) peak of the STF35 is clearly present. After exposure to 1200°C the peak at $2\theta = 31.6^\circ$ increased its intensity and after reaction at 1300°C it became the major peak apart from YSZ. This peak is attributed to the $\text{Sr}_3\text{Ti}_2\text{O}_7$ Ruddlesden-Popper phase. It has tetragonal (space group $I4mmm$) crystal structure. According to the JCPDS database (file number 11-663), its 100 % peak is at the position of $2\theta = 31.615^\circ$ and represents the (105) plane. Peaks from the STF35 phase are not visible after reaction at 1300°C. Beside the YSZ and $\text{Sr}_3\text{Ti}_2\text{O}_7$ no other phases are detected. Interestingly, the relative intensities of the peaks originating from the YSZ phase change with temperature. This is especially visible when comparing intensities of the (111) and (220) peak positions. The higher the temperature, the relative intensity of the (220) becomes stronger. The same occurs to the (311) peak intensity. For the STF50 and STF65 compositions, the reactions were very similar in character to the STF35 sample (diffractograms not presented here). Higher iron content resulted in intensified reaction between materials. Even after exposure to 1100°C reaction products were observed in XRD patterns with higher intensities than for STF35 sample. Chemical reaction of the slightly A-site deficient $\text{Sr}_{0.97}\text{Ti}_{0.6}\text{Fe}_{0.4}\text{O}_3$ with the YSZ was studied before by Fagg *et al.* [17]. Authors mixed YSZ and STF powder in 1:1 volume ratio and fired these powders at 1250°C for 12 hours. In their study a peak attributable to the reaction product was noticed and STF peak was still present. Although no attempt was made to describe this new phase, from the available patterns it might be found to be the same product as found in the present work. For the higher A-site deficiency sample, $\text{Sr}_{0.90}\text{Ti}_{0.6}\text{Fe}_{0.4}\text{O}_3$ the reaction has diminished greatly while for the $\text{La}_{0.4}\text{Sr}_{0.6}\text{Ti}_{0.6}\text{Fe}_{0.4}\text{O}_3$ composition no reaction between powders was found at all. It might be stated, that either introducing A-site deficiency or introducing La atoms into the A-site will reduce chemical reactivity between powders.

Typical impedance spectra of STF35, STF50 and STF65 symmetrical electrodes sintered at 1100°C and measured at 800°C are presented in Fig. 4. The shape of spectra resembles the spectra obtained for STF5 reported in [13]. For higher Fe content spectra differed from these, showing only one semicircle. A ohmic resistance is defined as a high frequency x-axis intercept, the polarisation resistance as a difference between low and high frequency intercepts:

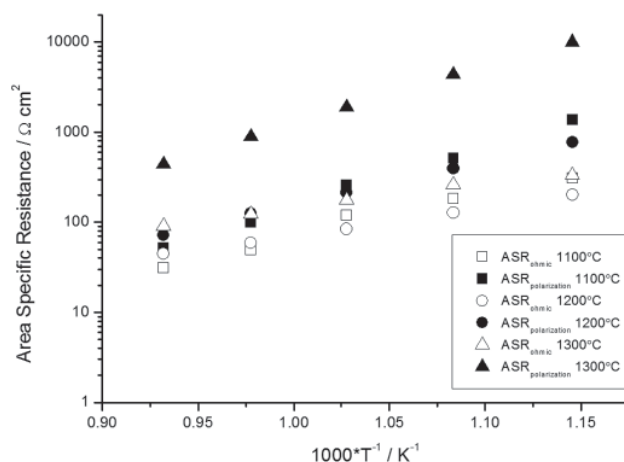


Fig. 5. Area Specific Resistance of a symmetrical STF35 electrode on YSZ electrolyte.

$$R_{ohmic} = R_{high_frequency} [\Omega], \quad (1)$$

$$R_{polarization} = R_{low_frequency} - R_{high_frequency} [\Omega]. \quad (2)$$

Results obtained for STF35 and STF63 reveal some common features. The ohmic resistances, which is usually attributed to the YSZ electrolyte, have a similar value. However, the resistance of about 80 Ω cannot be directly connected to the pure YSZ electrolyte. At this temperature, the YSZ alone should introduce approximately only 2-5 Ω to the overall results. The measured relatively high resistance thus can be probably connected to the chemical reaction between these materials, what results in a formation of some resistive phases on the interface. For STF50 the high frequency resistance is even higher, but the possible explanation remains the same.

Although the polarization part of the impedance is complex in shape, for the purpose of this paper it is only regarded as one resistance. As can be seen in Fig. 4. it consists of at least two overlapping semicircles, responsible for different physical or chemical processes. No attempt is made for the deconvolution of its complex shape into sub processes here, which will be the topic of further studies. To describe and compare electrode processes occurring in symmetrical cells an Area Specific Resistance is extensively used in the literature and defined as:

$$ASR = A \frac{R}{2} [\Omega \cdot \text{cm}^2], \quad (3)$$

where R is the resistance, A is the electrode area and the factor of 2 in the denominator is related to the fact, that on symmetrical cells one measures two identical interfaces between electrolyte and electrode. For the calculation of ASR values, both ohmic and polarization resistances were used. By this way two ASR parameters for each measurement were obtained.

Calculated Area Specific Resistances a function of temperature for STF35, STF50 and STF65 are presented in Figs. 5 and 7, respectively. In case of the STF35 (Fig. 5) the ohmic resistance is the smallest for the lowest processing temperature (1100°C) and the highest for the 1300°C sintered electrode. This would confirm the assumption, that this high resistance value is connected to the products of the reaction between YSZ and STF material. Polarization resistances present the same tendency with temperature.

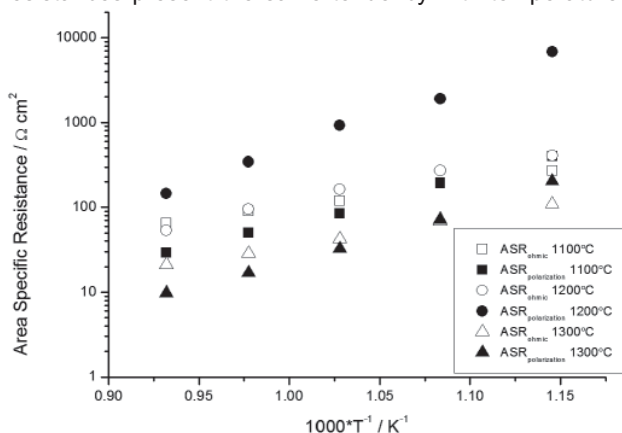


Fig. 6. Area Specific Resistance of a symmetrical STF50 electrode on YSZ electrolyte.

For the 1300°C sintered sample the polarization resistance is almost one order of magnitude higher than for the other two temperatures. Different behaviour was found for the STF50 composition (Fig. 6). In this case the increase of the processing temperature results in the enhanced performance. In other words, although the chemical interaction is the strongest in this temperature the electrochemical properties are improved. This might imply that to some extent the chemical reaction is not the main issue for this composition.

Table 2. Energies of activation and Area Specific Resistances obtained from Impedance Spectroscopy measurements.

Name:	Temp. [°C]	Type	E_a [eV]	$ASR_{800^\circ\text{C}}$ [Ωcm^2]
STF35	1100	Ohmic	0.95	31
		Polarization	1.32	52
	1200	Ohmic	0.61	44
		Polarization	0.96	71
	1300	Ohmic	0.54	90
		Polarization	1.26	440
STF50	1100	Ohmic	0.58	65
		Polarization	1.07	29
	1200	Ohmic	0.82	54
		Polarization	1.52	146
	1300	Ohmic	0.67	21
		Polarization	1.22	10
STF65	1100	Ohmic	0.82	37
		Polarization	1.39	77
	1200	Ohmic	0.70	58
		Polarization	1.29	196
	1300	Ohmic	0.75	140
		Polarization	1.31	32

The plots of calculated Area Specific Resistances (Figs. 5 and 7) in a function of temperature are linear. Therefore for all datasets activation energies related to Arrhenius type of conductivity were calculated. These together with ASR values measured at 800°C are presented in Table 2. As a general rule the activation energy of ASR_{ohmic} is smaller than that of $ASR_{polarization}$. The activation energies of ASR_{ohmic} alter between 0.54 eV for STF35 sintered at 1300°C to 0.95 eV for STF35 but sintered at 1100°C. In case of the $ASR_{polarization}$ activation energies alter between 0.96 eV for STF35 sintered at 1200°C and 1.52 eV for STF50 sintered at 1200°C. In the available literature, in the temperature range of 570-650°C the STF activation energy of 2.00 eV, 1.80 eV and 1.90 eV for STF35, STF50 and STF80 were obtained, respectively. In this case a one semicircle was observed in the impedance spectra and thus different processes can be considered. However authors noticed, that in low frequencies there is a sign of another contribution to the spectra, however, no attempt was made to clarify this. In this work the ohmic resistance (offset resistance) was attributed to the YSZ electrolyte material. In case of ohmic resistance the activation energy is lower than usually reported for the YSZ ceramics (~1 eV). Also the level of ASR_{ohmic} is too high to be attributed to the YSZ. In the case of the $ASR_{polarization}$ at

800°C the results are much higher than data presented by Jung *et al.* [13, 14]. The lowest $ASR_{polarization}$ value obtained at 800°C is 10 Ωcm^2 for the STF50 sintered at 1300°C. The highest value is 440 Ωcm^2 for STF35 sintered at 1300°C. In the [13, 14] polarization resistances for STF materials were as small as $\sim 3 \Omega\text{cm}^2$ at 650°C for STF80 sample. Interestingly, although electrical conductivities of STF materials differed greatly between them, this has no visible effect on the measured impedance spectra. There are several factors that can cause these negative effects. First of all, cathode materials used in this study are prepared from pastes and this result in porous layers after sintering. Electrical properties of dense and highly porous layers are much different. Electrical conductivity of dense materials can be more than an order of magnitude higher than for porous ones. Another important factor is high temperature used to sinter cathode materials on the electrolyte surface. This results in the chemical reaction between YSZ-STF and end-up in a lowered electrochemical performance. In [13, 14], the authors deposited dense STF layers by the PLD method, which is a low-temperature method of deposition. In their case, the substrate was heated to a temperature of 700°C and was the maximum sample processing temperature throughout the studies. At such low temperature chemical interaction is very limited.

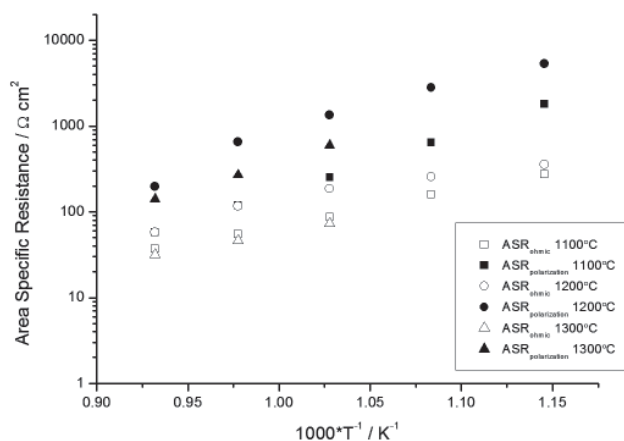


Fig. 7. Area Specific Resistance of a symmetrical STF65 electrode on YSZ electrolyte.

4. Conclusions

In this paper iron doped strontium titanate powders were synthesized. A two stage preparation route was needed to obtain phase pure powders with desired properties. Electrical conductivity showed a zero-TCR parameter for the STF35 composition. The level of the electrical conductivity differed for more than an order of magnitude between synthesised materials. The chemical reactivity between YSZ and STF materials was studied in the temperature range of 1100-1300°C. Results show, that for the STF35 the reaction between perovskite and YSZ is only minor, while for other compositions is higher. Area Specific Resistances of prepared electrodes were very high, with the best result of $\sim 10 \Omega\text{cm}^2$ at 800°C for the STF50 sample sintered at 1300°C. This is much higher than reported for dense thin-film model electrodes and probably caused by the porous nature of the electrode and chemical interaction between electrode and electrolyte

material. Unfortunately, obtained results do not make these materials promising as SOFCs' cathodes when conventional high temperature fabrication methods are applied. However, superior physicochemical properties demonstrated before still offer potential advantages to be exploited in future.

Acknowledgment

This work is supported by the Polish Ministry of Science and Higher Education under the project N N511 376135.

References

- [1] Dokiya M.: Solid State Ionics, 152-153, (2002), 383-392.
- [2] Beckel D., Bieberle-Hütter A., Harvey A., Infortuna A., Muecke U., Prestat M., Rupp J., Gauckler L.: J. Power Sources, 173, (2007), 325-345.
- [3] Adler S.B.: Chemical Reviews, 104, (2004), 4791-4844.
- [4] Jiang S.: J. Mater. Sci., 43, (2008), 6799-6833.
- [5] Meyer R., Waser R.: Sensors & Actuators: B. Chemical, 101, (2004), 335-345.
- [6] Abrantes J.C.C., Feighery A., Ferreira A.A.L., Labrincha J.A., Frade J.R.: J. Am. Ceram. Soc., 85, (2002), 2745-2752.
- [7] Blennow P., Hansen K.K., Wallenberg L.R., Mogensen M.: Solid State Ionics, (2008), doi:10.1016/j.ssi.2008.10.011
- [8] Blennow P., Hagen A., Hansen K.K., Wallenberg L.R., Mogensen M.: Solid State Ionics, 179, (2008), 2047-2058.
- [9] Karczewski J., Riegel B., Molin S., Winiarski A., M. Gazda, Jasinski P., Murawski L., Kusz B.: J. Alloys Compd, 473, (2009) 496-499.
- [10] Menesklou W., Schreiner H., Härdtl K.H., Ivers-Tiffée E.: Sensors and Actuators B: Chemical, 59, (1999), 184-189.
- [11] Sahner K., Moos R., Izu N., Shin W., Murayama N.: Sensors & Actuators: B. Chemical, 113, (2006), 112-119.
- [12] Meuffels P.: Journal of the European Ceramic Society, 27, (2007), 285-290.
- [13] Jung W.C., Tuller H.L.: Solid State Ionics, (2009), doi:10.1016/j.ssi.2009.02.008
- [14] Jung W.C., Tuller H.L.: J Electrochem. Soc., 155, (2008), B1194.
- [15] Jiang S.P.: Solid State Ionics, 146, (2002), 1-22.
- [16] Zhou W., Ran R., Shao Z.: J. Power Sources, 192, (2009), 231-246.
- [17] Fagg D.: J. Eur. Ceram. Soc., 21, (2001), 1831-1835.
- [18] Neri G., Bonavita A., Micali G., Rizzo G., Licheri R., Orrù R., Cao G.: Sensors and Actuators B: Chemical, 126, (2007), 258-265.
- [19] Rothschild A., Litzelman S.J., Tuller H.L., Menesklou W., Schneider T., Ivers-Tiffée E.: Sensors and Actuators B: Chemical, 108, (2005), 223-230.
- [20] Neri G., Micali G., Bonavita A., Licheri R., Orrù R., Cao G., Marzorati D., Merlone Borla E., Roncari E., Sanson A., Sensors and Actuators B: Chemical, 134, (2008), 647-653.

Received 1 March 2010; accepted 8 May 2010